Reduced nitric oxide bioavailability mediates cerebroarterial dysfunction independent of cerebral amyloid angiopathy in a mouse model of Alzheimer's disease

Merlini, Mario ; Shi, Yi ; Keller, Stephan ; Savarese, Gianluigi ; Akhmedov, Alexander ; Derungs, Rebecca ; Spescha, Remo D ; Kulic, Luka ; Nitsch, Roger M ; Luescher, Thomas F ; Camici, Giovanni G

Abstract: In Alzheimer's disease (AD), cerebral arteries, in contrast to cerebral microvessels, show both cerebral amyloid angiopathy- (CAA) dependent and -independent vessel wall pathology. However, it remains unclear whether CAA-independent vessel wall pathology affects arterial function thereby chronically reducing cerebral perfusion, and if so which mechanisms mediate this effect. To this end, we assessed the ex vivo vascular function of the basilar artery and a similar-sized peripheral artery (femoral artery) in the Swedish-Arctic (SweArc) transgenic AD mouse model at different disease stages. Further, we used quantitative immunohistochemistry to analyze CAA, endothelial morphology, and molecular pathways pertinent to vascular relaxation. We found that endothelium-dependent, but not smooth muscle-dependent vasorelaxation was significantly impaired in basilar and femoral arteries of 15-month-old SweArc mice compared to that of age-matched wildtype (WT) and 6-month-old SweArc mice. This impairment was accompanied by significantly reduced levels of cyclic GMP (cGMP), indicating a reduced nitric oxide (NO) bioavailability. However, no age- and genotype-related differences in oxidative stress as measured by lipid peroxidation were observed. Although parenchymal capillaries, arterioles, and arteries showed abundant CAA in the 15-month-old SweArc mice, no CAA or changes in endothelial morphology were detected histologically in the basilar and femoral artery. Thus, our results suggest that in this AD mouse model dysfunction of large intracranial, extracerebral arteries important for brain perfusion is mediated by reduced NO bioavailability rather than by CAA. This finding supports the growing body of evidence highlighting the therapeutic importance of targeting the cerebrovasculature in AD.

DOI: https://doi.org/10.1152/ajpheart.00607.2016

Articles in PresS. Am J Physiol Heart Circ Physiol (December 6, 2016). doi:10.1152/ajpheart.00607.2016

Reduced nitric oxide bioavailability mediates cerebroarterial dysfunction independent of cerebral amyloid angiopathy in a mouse model of Alzheimer's disease

Mario Merlini[*1,2], Yi Shi[*3], Stephan Keller[1], Gianluigi Savarese[4], Alexander Akhmedov[1], Rebecca Derungs[5], Remo D. Spescha[1], Luka Kulic[2,5], Roger M. Nitsch[2,5], Thomas F. Lüscher[1] and Giovanni G. Camici[1,2]

1) Center for Molecular Cardiology, Schlieren, University of Zurich and Department of Cardiology, University Heart Center, University Hospital Zurich, Switzerland; 2) Neuroscience Center Zurich – ZNZ; 3) Biomedical Research Center, Zhongshan Hospital, Fudan University, Shanghai, China; 4) Department of Medicine, Karolinska University Hospital, Stockholm, Sweden; 5) Institute for Regenerative Medicine – IREM, University of Zurich, Schlieren, Switzerland

[*]These authors contributed equally to this work

Running head: Cerebroarterial dysfunction in SweArc AD mice

Correspondence to:

Giovanni G. Camici, PhD

Center for Molecular Cardiology, University of Zurich

Wagistrasse 12, CH-8952 Schlieren, Switzerland

Email: giovanni.camici@uzh.ch

Phone +41 44 635 64 68, Fax +41 44 635 68 27

ABSTRACT

In Alzheimer's disease (AD), cerebral arteries, in contrast to cerebral microvessels, show both cerebral amyloid angiopathy- (CAA) dependent and -independent vessel wall pathology. However, it remains unclear whether CAA-independent vessel wall pathology affects arterial function thereby chronically reducing cerebral perfusion, and if so which mechanisms mediate this effect. To this end, we assessed the *ex vivo* vascular function of the basilar artery and a similar-sized peripheral artery (femoral artery) in the Swedish-Arctic (SweArc) transgenic AD mouse model at different disease stages. Further, we used quantitative immunohistochemistry to analyze CAA, endothelial morphology, and molecular pathways pertinent to vascular relaxation. We found that endothelium-dependent, but not smooth muscle-dependent vasorelaxation was significantly impaired in basilar and femoral arteries of 15-month-old SweArc mice compared to that of age-matched wildtype (WT) and 6-month-old SweArc mice. This impairment was accompanied by significantly reduced levels of cyclic GMP (cGMP), indicating a reduced nitric oxide (NO) bioavailability. However, no age- and genotype-related differences in oxidative stress as measured by lipid peroxidation were observed. Although parenchymal capillaries, arterioles, and arteries showed abundant CAA in the 15-month-old SweArc mice, no CAA or changes in endothelial morphology were detected histologically in the basilar and femoral artery. Thus, our results suggest that in this AD mouse model dysfunction of large intracranial, extracerebral arteries important for brain perfusion is mediated by reduced NO bioavailability rather than by CAA. This finding supports the growing body of evidence highlighting the therapeutic importance of targeting the cerebrovasculature in AD.

Keywords: Alzheimer's disease; cerebral amyloid angiopathy; cerebrovascular pathology; endothelial dysfunction; nitric oxide; cyclic GMP

52

NEW & NOTEWORTHY

We show that vasorelaxation of the basilar artery—a large intracranial, extracerebral artery important for cerebral perfusion—is impaired independent of cerebral amyloid angiopathy in a transgenic mouse model of Alzheimer's disease. Interestingly, this dysfunction is specifically endothelium-related and is mediated by impaired nitric oxide–cyclic GMP bioavailability.

INTRODUCTION

Cerebrovascular pathology is inherent to Alzheimer's disease (AD), with several lines of evidence indicating that it also strongly contributes to the onset of the disease (1, 2, 4). However, the molecular mechanisms underlying cerebrovascular pathogenesis at the different AD stages remain unknown. Vascular amyloid β (Aβ) deposition, known as cerebral amyloid angiopathy (CAA), severely affects cerebrovascular functionality and instigates a plethora of vascular abnormalities that play critical roles in the onset and progression of AD. These include vasculitis, vascular smooth muscle cell (VSMC) loss, and blood-brain barrier (BBB) leakage (10, 12, 17, 29, 30). However, pathologic remodeling of cerebral arteries is also observed prior to onset of AD in the absence of CAA, indicating that CAA certainly exacerbates cerebrovascular pathology but is not required to initiate it (18, 21). Thus, investigating CAA-independent changes in the functionality of cerebral vessels in AD is important for the early diagnosis of the disease.

Soluble oligomeric Aβ species decrease the vasodynamic capacity of cerebral penetrating arterioles, independent of the presence of CAA (6). Whether VSMC and/or endothelial cell functionality in the upstream, major intracranial cerebral arteries may be impaired in the absence of CAA as well is, however, not clearly delineated. Therefore, herein, we recorded endothelium-dependent and -independent *ex vivo* vasodilatation and -constriction of the basilar artery in a transgenic mouse model of amyloidosis harboring the human Swedish and Arctic AD double mutation (SweArc mice) (20). This mouse model is characterized by progressive age-dependent cerebrovascular pathology, soluble oligomeric Aβ species generation (13, 14, 16, 17), and cerebral hypoperfusion both before and after CAA onset (14, 17, 22). Additionally, we performed quantitative histological assessments of endothelial morphology, lipid peroxidation as a marker of oxidative stress, CAA, and cyclic GMP (cGMP) as a readout of nitric oxide bioavailability. We used 6- and 15-month old SweArc and wildtype (WT) mice to discern age- from CAA-dependent mechanisms that

affect cerebral arterial function. So as to have a systemic artery control, we compared basilar artery relaxation to that of the similarly sized femoral artery. Using this experimental approach, we tested the hypothesis that dysfunction of large cerebral arteries in AD can also occur in the absence of CAA.

MATERIALS AND METHODS

Animals

The basilar artery and distal portion of the femoral artery were isolated from 6- and 15-month-old male SweArc mice (n = 8/age group) and their WT littermates (n = 7/age group) (C57Bl6/J background). Mice were housed under OHB conditions at the Laboratory Animal Services Center (LASC) of the University of Zurich (Zurich, Switzerland), with access to regular chow and water *ad libitum*. On the day of the experiments, mice were euthanized with carbon dioxide. All procedures and protocols were approved by the Veterinary Department (BVET; Swiss Animal Welfare Act, 2008, no. 455) of the Canton of Zurich and were performed according to the BVET guidelines.

Organ chamber recordings

Organ chamber recordings were performed non-blinded as previously described (26). Briefly, the femoral and basilar artery of the mice were dissected, excised, and placed in ice-cold modified Krebs–Ringer solution (in mmol/L: NaCl 118, KCl 4.7, $CaCl_2$ 2.5, $MgSO_4$ 1.2, $NaHCO_3$ 25.0, KH_2PO_4 1.18, calcium disodium EDTA 0.026, and glucose 11.1). Arterial rings were cut (0.8–1.4 mm in length, $n \geq 3$/recording) and mounted in organ chambers containing Krebs-Ringer solution (37°C) aerated with 95% O_2 and 5% of CO_2, which were connected to a force transducer (M610 DMT, Inc., Denmark). The rings were stretched progressively to their optimal resting tension according to the manufacturer's protocol.

Internal circumference of the arteries was determined corresponding to a transmural pressure of 100 mmHg. The diameter of the artery was calculated according to its internal circumference. Changes in tension were expressed as a percentage of the reference contraction to U46619, a thromboxane A2 receptor agonist, obtained at the beginning of the experiment. Artery ring recordings were acquired in the presence of sodium nitroprusside (SNP) or acetylcholine (Ach) to study endothelium-independent and -dependent relaxation in a concentration–dependent manner.

Histology

Histological procedures were performed as previously described (17). Briefly, following induction of deep anesthesia, mice were transcardially perfused with phosphate-buffered saline (PBS) and 4.0% paraformaldehyde (PFA) in PBS at room temperature, followed by incubation in 30% sucrose in PBS for 36 h. Cryoprotected brains were cut into 35-µm thick free-floating sections, and were pretreated with proteinase K for antigen retrieval, immune-blocked, and incubated overnight at 4°C with an antibody against Aβ (purified mouse 6E10, 1:1000; Covance/Signet, SIG-39300), the endothelial marker CD31 (rat anti-CD31/PECAM1, 1:50; BD Pharmingen, 553370), the VSMC marker alpha-smooth muscle actin (alpha-SMA) (goat anti-alpha-SMA, 1:250; Abcam, ab21027), cGMP (sheep anti-cGMP, 1:150; BioRad, OBT5055), and/or the lipid peroxidation marker 4-hydroxynonenal (4-HNE) (rabbit anti-4-HNE, 1:200; Abcam, ab46545). The brain sections were subsequently incubated with secondary antibodies (a combination of either Alexa488-conjugated donkey anti-rat IgG [1:750], Alexa594-conjugated donkey anti-goat IgG [1:750], and Alexa647-conjugated donkey anti-mouse IgG [1:500] or Alexa488-conjugated donkey anti-rat IgG [1:750], Alexa546-conjugated donkey anti-sheep [1:750], and Alexa405-conjugated donkey anti-rabbit [1:750]; Jackson ImmunoResearch, Suffolk, UK) for 2 h at RT. Images were acquired in sequential mode and at a 1-µm step size interval using a confocal

157 microscope (Leica SP8; Leica, Wetzlar, Germany). They were processed as maximum
158 projection z-stacks in Image J (National Institutes of Health, Bethesda, MA, USA) and were
159 analyzed using an in-house generated MATLAB script based on the Imaging Toolbox of
160 MATLAB (v2016b; MathWorks, Natick, MA, USA).
161
162 *Statistical analyses*
163 The data are presented as the mean ± SEM. For the artery ring experiments, two-way
164 ANOVA followed by Bonferroni's post-hoc comparison test was used; the histological data
165 were analyzed using a two-tailed, nonparametric (Mann–Whitney) Student's *t*-test (GraphPad
166 Prism, version 7; GraphPad Software, La Jolla, CA, USA). Differences were considered
167 statistically significant at $p < 0.05$.
168
169
170

RESULTS

General physiological parameters were assessed in the SweArc and WT mice to confirm comparable conditions in the two genotypes. As shown in Figure 1A, the diameter of the femoral and basilar artery was comparable in the SweArc and WT mice at both 6- and 15-months of age, with an average luminal diameter of ~170 μm (6-month-old) and ~150 μm (15-month-old) for the femoral artery, and ~150 μm (6- and 15-month-old) for the basilar artery. Likewise, the resting tension of the femoral and basilar artery was similar between and among the 6- and 15-month-old SweArc and WT mice (~1.1 mN) (Fig. 1A). Body and heart weight in the 6-month-old mice was 29.8 ± 9.3 g and 0.13 ± 0.03 (SweArc), and 32.8 ± 7.1 g and 0.15 ± 0.03 g (WT), respectively; in the 15-month-old mice it was equal to 37.7 ± 11.2 g and 0.18 ± 0.04 g (SweArc), and 44.9 ± 7.9 g and 0.19 ± 0.03 g (WT), respectively.

Next, we assessed endothelium- and VSMC-dependent vasorelaxation after U46619-induced pre-contraction using acetylcholine and sodium nitroprusside (SNP), respectively (26). No significant differences in endothelium-dependent and –independent relaxation were observed between the two artery types of 6-month-old WT and SweArc mice (Fig. 1B). In contrast, femoral arteries of 15-month-old SweArc mice showed a significant decrease in endothelium-dependent relaxation compared to that of age-matched WT mice (AUC WT and SweArc: 851 ± 31.2 and 603 ± 30.5, respectively; $p < 0.001$) (Fig. 1C). This difference was exacerbated in the basilar artery of 15-month-old SweArc mice, showing a paradoxical vasoconstriction as opposed to the expected vasodilatation observed in the age-matched WT mice (AUC WT and SweArc: 778 ± 26.1 and 384 ± 69.7, respectively; $p < 0.001$). Endothelium-independent relaxation, on the other hand, was similar between the aged SweArc and WT mice (Fig. 1C).

Given the specific impairment in Ach-induced, NO-mediated vasorelaxation with a paradoxical vasoconstriction observed in the 15-month-old SweArc mice, we assessed whether this might be related to reduced levels of cGMP, a marker of NO bioavailability.

Indeed, quantitative histological analysis of cGMP in free-floating brain sections containing the basilar artery showed a significant decrease in cGMP in the 15-month-old SweArc mice compared to that in age-matched WT littermate controls and in 6-month-old SweArc and WT mice (Fig. 2A–E). In line with the comparable Ach-induced vasorelaxation in the 6-month-old SweArc and WT mice, no significant differences in basilar artery cGMP levels were observed between these two groups. Further, no effect of aging on cGMP levels was observed in either the WT or SweArc mice (Fig. 2E).

Aβ may increase reactive oxygen species (ROS) levels (24), thereby scavenging NO and diminishing its bioavailability (7). However, staining of the basilar artery for 4-HNE, a marker of lipid peroxidation and, thus, of oxidative stress, revealed equally low signals in both strains irrespective of age (Fig. 2A–E). This suggests that the observed reduced bioavailability of NO is not related to an increased scavenging by free radicals but perhaps to decreased NO production. Similarly, quantitative analysis of hyperplastic and/or hypertrophic changes in the endothelial cells of the SweArc basilar arteries that might underlie the observed decrease in cGMP showed no significant differences in these parameters between the SweArc and WT basilar arteries (Fig. 3A–C). These data confirmed that the differences observed were independent of morphological changes in the basilar artery endothelium.

As we have previously shown, penetrating and intraparenchymal microvessels and arteries of SweArc mice show widespread CAA starting at around 8 months of age, which increases in severity with advancing age and has detrimental effects on the vasculature (14, 17). In line with the above, staining for Aβ confirmed that the intraparenchymal vessels were affected by CAA in the 15-month-old SweArc mice (Fig. 4A); however, CAA was absent in the basilar artery (Fig. 4B) similar to the complete absence of parenchymal Aβ and CAA in the 15-month-old WT littermate controls (Fig. 4C and D). Of note, Aβ deposition in the vessel wall of peripheral arteries and microvessels is not observed in SweArc mice.

DISCUSSION

We assessed systemic versus cerebral vascular function in a mouse model Alzheimer's disease (AD) at different disease stages. We found CAA-independent endothelial dysfunction and reduced NO bioavailability, which was particularly accentuated in the basilar artery whereby paradoxical vasoconstrictions in response to Ach were observed. These findings may increase the understanding of the vascular pathology and related chronic cerebral hypoperfusion present at pre-AD stages where CAA is rare (9, 15, 23). Further, our findings are in line with our previous histological studies in human brain and those of others showing CAA-independent pathologic remodeling of vessel wall constituents regulating arterial vasodynamics (18, 21).

Our finding of a histological reduction in cGMP content along with impairment in Ach-induced vasorelaxation in the basilar artery of 15-month-old SweArc mice, is in line with that of another study (19). Although there the authors had not assessed vasodynamic responses as we did, they showed that both soluble and fibrillar Aβ impaired NO–cGMP signaling by inhibiting the activation of guanylate cyclase. Both these forms of Aβ are abundantly present in aged SweArc mice (14). Indeed, soluble protofibrillar Aβ species increase in an age-dependent manner in SweArc mice, specifically from 8 months onward (16, 25), potentially explaining the unchanged basilar artery cGMP content and conserved responses to Ach in 6-month-old SweArc mice.

Given the absence of CAA in the basilar artery and the fact that the femoral artery also showed impaired endothelium-dependent relaxation, soluble Aβ species rather than CAA may be considered the key trigger of endothelial dysfunction in large cerebral arteries as observed in the 15-month-old SweArc mice. Soluble Aβ species are produced by VSMCs as well as neurons (8); the ones produced by the latter can also reach the vascular system through perivascular drainage routes (11, 12). Thus, the high level of soluble Aβ species observed in old SweArc mice combined with the vessel-directed Aβ clearance routes causes chronic

exposure of the vessel wall to high levels of toxic soluble Aβ species which, consequently, may alter NO levels (6). Nevertheless, despite this high vessel wall exposure to soluble Aβ, the VSMC-dependent responses to SNP were comparable in wild type and SweArc mice, irrespective of age. This is in contrast to what we and others have previously shown for the deleterious effect of CAA on VSMC function and morphology (17, 18, 28).

Our results indicate that, at least for the endothelium of the basilar and femoral artery, CAA is not a prerequisite for inducing endothelial dysfunction. However, although we did not detect CAA in the basilar artery, pathologic changes in the CAA-affected leptomeningeal and intraparenchymal vessels downstream of the basilar artery could still partially contribute to the observed vascular dysfunction as they are known to affect vascular integrity and function over large distances (5). Moreover, histological detection of vascular-related Aβ/CAA lacks the sensitivity that biochemical assays have for detecting (soluble) Aβ species in the vessel wall, thereby providing a limited assessment of the actual total vessel wall Aβ content (27).

Aging per se impairs cerebrovascular function; therefore, cerebrovascular impairment due to aging and/or to AD pathology needs careful delineation. We previously showed age-related impairment of endothelium-dependent basilar artery relaxation in WT mice (26). Thus, the similarly blunted vasorelaxation observed in the basilar artery of 6-month-old SweArc and 6- and 15-month-old WT mice in the present study is most likely an effect of aging. However, the exacerbated arterial dysfunction with a paradoxical vasoconstriction observed in 15-month-old SweArc mice indicates a combined effect of aging and Aβ-mediated reduction in NO bioavailability.

SweArc mice, like other transgenic AD mice, only partially model aspects of the vast cerebrovascular pathology that is present in AD (2), thus posing limits to the extrapolation of our results to the disease in humans. Nevertheless, taken together, our data add to the growing understanding of the multi-faceted vascular insults that contribute to AD (2, 3, 18). They especially shed much needed light on the functional implications of cerebrovascular

pathology in AD, and provide further evidence of the need for vascular-specific therapies to combat this disease.

ACKNOWLEDGEMENTS

We are grateful to Dr. Maria Teresa Ferretti, Institute for Regenerative Medicine – IREM, University of Zurich, Switzerland, for providing the SweArc and WT littermate control mice.

FUNDING

This study was supported by the Swiss National Science Foundation (310030_147017, to GGC), Grants for Translational and Clinical Research Cardiology and Oncology Alfred and Annemarie von Sick Grants, Zurich (to GGC), and National Natural Science Foundation of China 81573418 (to YS).

DISCLOSURES

Roger M. Nitsch owns stock in Neurimmune Therapeutics AG, Switzerland, and is co-founder and member of the board of directors of said company.

AUTHOR CONTRIBUTIONS

YS and MM performed the experiments and acquired the data; SK provided technical assistance with the organ chamber recordings; MM wrote the manuscript with the contribution of YS and GGC; GGC, YS, LK, and MM designed the experiments and analyzed the data; RD, RS, GS, AA, and LK contributed to the experiments; RN and TFL gave fundamental intellectual input for the study design and data interpretation; all authors read and edited the manuscript.

301

REFERENCES

1. **Attems J, Jellinger KA.** The overlap between vascular disease and Alzheimer's disease--lessons from pathology. *BMC Med* 12: 206, 2014.

2. **Carare RO, Kalaria R.** Cerebrovascular pathology: the dark side of neurodegeneration. *Acta Neuropathol* 131: 641-643, 2016.

3. **Corriveau RA, Bosetti F, Emr M, Gladman JT, Koenig JI, Moy CS, Pahigiannis K, Waddy SP, Koroshetz W.** The science of vascular contributions to cognitive impairment and dementia (VCID): A framework for advancing research priorities in the cerebrovascular biology of cognitive decline. *Cell Mol Neurobiol* 36: 281-288, 2016.

4. **Csiszar A, Tucsek Z, Toth P, Sosnowska D, Gautam T, Koller A, Deak F, Sonntag WE, Ungvari Z.** Synergistic effects of hypertension and aging on cognitive function and hippocampal expression of genes involved in beta-amyloid generation and Alzheimer's disease. *Am J Physiol Heart Circ Physiol* 305: H1120-1130, 2013.

5. **Di Marco LY, Farkas E, Martin C, Venneri A, Frangi AF.** Is vasomotion in cerebral arteries impaired in Alzheimer's disease? *J Alzheimers Dis* 46: 35-53, 2015.

6. **Dietrich HH, Xiang C, Han BH, Zipfel GJ, Holtzman DM.** Soluble amyloid-beta, effect on cerebral arteriolar regulation and vascular cells. *Mol Neurodegener* 5: 15, 2010.

7. **Faraci FM.** Protecting against vascular disease in brain. *Am J Physiol Heart Circ Physiol* 300: H1566-1582, 2011.

8. **Frackowiak J, Zoltowska A, Wisniewski HM.** Non-fibrillar beta-amyloid protein is associated with smooth muscle cells of vessel walls in Alzheimer disease. *J Neuropathol Exp Neurol* 53: 637-645, 1994.

9. **Gommer ED, Martens EG, Aalten P, Shijaku E, Verhey FR, Mess WH, Ramakers IH, Reulen JP.** Dynamic cerebral autoregulation in subjects with Alzheimer's

disease, mild cognitive impairment, and controls: evidence for increased peripheral vascular resistance with possible predictive value. *J Alzheimers Dis* 30: 805-813, 2012.

10. **Gurol ME, Greenberg SM.** A physiologic biomarker for cerebral amyloid angiopathy. *Neurology* 81: 1650-1651, 2013.

11. **Hawkes CA, Sullivan PM, Hands S, Weller RO, Nicoll JA, Carare RO.** Disruption of arterial perivascular drainage of amyloid-beta from the brains of mice expressing the human APOE epsilon4 allele. *PLoS One* 7: e41636, 2012.

12. **Keable A, Fenna K, Yuen HM, Johnston DA, Smyth NR, Smith C, Al-Shahi Salman R, Samarasekera N, Nicoll JA, Attems J, Kalaria RN, Weller RO, Carare RO.** Deposition of amyloid beta in the walls of human leptomeningeal arteries in relation to perivascular drainage pathways in cerebral amyloid angiopathy. *Biochim Biophys Acta* 1862: 1037-1046, 2016.

13. **Knobloch M, Farinelli M, Konietzko U, Nitsch RM, Mansuy IM.** Abeta oligomer-mediated long-term potentiation impairment involves protein phosphatase 1-dependent mechanisms. *J Neurosci* 27: 7648-7653, 2007.

14. **Knobloch M, Konietzko U, Krebs DC, Nitsch RM.** Intracellular Abeta and cognitive deficits precede beta-amyloid deposition in transgenic arcAbeta mice. *Neurobiol Aging* 28: 1297-1306, 2007.

15. **Liu J, Zhu YS, Khan MA, Brunk E, Martin-Cook K, Weiner MF, Cullum CM, Lu H, Levine BD, Diaz-Arrastia R, Zhang R.** Global brain hypoperfusion and oxygenation in amnestic mild cognitive impairment. *Alzheimers Dement* 10: 162-170, 2014.

16. **Lord A, Englund H, Soderberg L, Tucker S, Clausen F, Hillered L, Gordon M, Morgan D, Lannfelt L, Pettersson FE, Nilsson LN.** Amyloid-beta protofibril levels correlate with spatial learning in Arctic Alzheimer's disease transgenic mice. *FEBS J* 276: 995-1006, 2009.

17. **Merlini M, Meyer EP, Ulmann-Schuler A, Nitsch RM.** Vascular beta-amyloid and early astrocyte alterations impair cerebrovascular function and cerebral metabolism in transgenic arcAbeta mice. *Acta Neuropathol* 122: 293-311, 2011.

18. **Merlini M, Wanner D, Nitsch RM.** Tau pathology-dependent remodelling of cerebral arteries precedes Alzheimer's disease-related microvascular cerebral amyloid angiopathy. *Acta Neuropathol* 131: 737-752, 2016.

19. **Miller TW, Isenberg JS, Shih HB, Wang Y, Roberts DD.** Amyloid-beta inhibits No-cGMP signaling in a CD36- and CD47-dependent manner. *PLoS One* 5: e15686, 2010.

20. **Nilsberth C, Westlind-Danielsson A, Eckman CB, Condron MM, Axelman K, Forsell C, Stenh C, Luthman J, Teplow DB, Younkin SG, Naslund J, Lannfelt L.** The 'Arctic' APP mutation (E693G) causes Alzheimer's disease by enhanced Abeta protofibril formation. *Nat Neurosci* 4: 887-893, 2001.

21. **Perry G, Smith MA, McCann CE, Siedlak SL, Jones PK, Friedland RP.** Cerebrovascular muscle atrophy is a feature of Alzheimer's disease. *Brain Res* 791: 63-66, 1998.

22. **Ronnback A, Zhu S, Dillner K, Aoki M, Lilius L, Naslund J, Winblad B, Graff C.** Progressive neuropathology and cognitive decline in a single Arctic APP transgenic mouse model. *Neurobiol Aging* 32: 280-292, 2011.

23. **Ruitenberg A, den Heijer T, Bakker SL, van Swieten JC, Koudstaal PJ, Hofman A, Breteler MM.** Cerebral hypoperfusion and clinical onset of dementia: the Rotterdam Study. *Ann Neurol* 57: 789-794, 2005.

24. **Schilling T, Eder C.** Amyloid-beta-induced reactive oxygen species production and priming are differentially regulated by ion channels in microglia. *J Cell Physiol* 226: 3295-3302, 2011.

25. **Sehlin D, Fang XT, Cato L, Antoni G, Lannfelt L, Syvanen S.** Antibody-based PET imaging of amyloid beta in mouse models of Alzheimer's disease. *Nat Commun* 7: 10759, 2016.

26. **Shi Y, Savarese G, Perrone-Filardi P, Luscher TF, Camici GG.** Enhanced age-dependent cerebrovascular dysfunction is mediated by adaptor protein p66Shc. *Int J Cardiol* 175: 446-450, 2014.

27. **Shinkai Y, Yoshimura M, Ito Y, Odaka A, Suzuki N, Yanagisawa K, Ihara Y.** Amyloid beta-proteins 1-40 and 1-42(43) in the soluble fraction of extra- and intracranial blood vessels. *Ann Neurol* 38: 421-428, 1995.

28. **Stopa EG, Butala P, Salloway S, Johanson CE, Gonzalez L, Tavares R, Hovanesian V, Hulette CM, Vitek MP, Cohen RA.** Cerebral cortical arteriolar angiopathy, vascular beta-amyloid, smooth muscle actin, Braak stage, and APOE genotype. *Stroke* 39: 814-821, 2008.

29. **Thal DR, Griffin WS, de Vos RA, Ghebremedhin E.** Cerebral amyloid angiopathy and its relationship to Alzheimer's disease. *Acta Neuropathol* 115: 599-609, 2008.

30. **Weller RO, Preston SD, Subash M, Carare RO.** Cerebral amyloid angiopathy in the aetiology and immunotherapy of Alzheimer disease. *Alzheimers Res Ther* 1: 6, 2009.

401 **FIGURE LEGENDS**

402 **Fig. 1.** General conditions and endothelium- and smooth muscle-mediated arterial relaxation
403 of Swedish-Arctic and wildtype littermate control mice. *A*: Graphs representing the diameter
404 and resting tension of the femoral and basilar artery of 15-month-old Swedish-Arctic
405 (SweArc, $n = 7$) and wildtype (WT, $n = 8$) littermate controls. No significant changes in any
406 of the parameters measured are observed between the two genotypes. *B*: Graphs showing the
407 absence of significant differences in endothelium-dependent (acetylcholine- [Ach] induced)
408 and vascular smooth muscle-dependent (sodium nitroprusside- (SNP) induced) relaxation
409 between the basilar and femoral artery of 6-month-old SweArc ($n = 7$) and WT mice ($n = 8$)
410 (artery rings: $n \geq 3$/recording). *C*: Graphs showing a significant reduction in endothelium-
411 dependent relaxation of the femoral and basilar artery of 15-month-old SweArc mice as
412 compared to that of their WT littermate controls. *B* and *C*: Smooth muscle-dependent
413 relaxation is not affected in the 15-month-old SweArc mice. $^{***}p < 0.001$, referring to AUC.
414

415 **Fig. 2.** Histological assessment of changes in the endothelial nitric oxide production marker
416 cyclic GMP (cGMP) and of the presence of lipid peroxidation/oxidative stress in the basilar
417 artery. *A–D*: Representative images of free-floating brain tissue sections at the level of the
418 basilar artery of a 6- and 15-month-old wildtype (WT) littermate control and 6- and 15-
419 month-old Swedish-Arctic (SweArc) mouse stained for the endothelial cell marker CD31
420 (green), cGMP (red), and the lipid peroxidation/oxidative stress marker 4-hydroxynonenal (4-
421 HNE). *E*: Quantification of the cGMP staining calculated as percentage of the CD31 staining
422 shows a significant decrease in cGMP in the basilar artery of 15-month-old SweArc mice ($n =$
423 5) compared to that in the basilar artery of 15-month-old WT littermates ($n = 4$), and of 6-
424 month-old WT ($n = 3$) and SweArc mice ($n = 3$). The percentage 4-HNE staining is equally
425 low between the different groups. Scale bar in *A* and *C* = 50 µm. $^{**}p < 0.01$, $^{***}p < 0.001$.

Fig. 3. Analysis of the number of endothelial cells and their morphology in the basilar artery. *A*: Representative images of free-floating brain tissue sections at the level of the basilar artery of a 15-month-old Swedish-Arctic (SweArc) and wildtype (WT) littermate control mouse stained for the endothelial cell marker CD31 (green). *B*: Quantification of the number of endothelial cells in five consecutive basilar artery sections of three SweArc and three WT mice reveals the absence of significant differences herein between the SweArc and WT littermate control mice. *C*: Similarly, no significant differences are observed in endothelial cell width between 15-month-old SweArc and WT littermate control mice. Scale bar in *A* = 50 μm.

Fig. 4. Distribution of cerebral amyloid angiopathy (CAA) in aged Swedish-Arctic mice and the absence of CAA and parenchymal amyloid β (Aβ) in wildtype (WT) littermate controls. *A*: Representative images showing the presence and wide-spread distribution of CAA-affected parenchymal arterioles (asterisk) and CAA-affected (penetrating) arteries (arrows) in the cortex of a 15-month-old SweArc mouse (CAA, red; CD31, green; alpha-smooth muscle actin [alpha-SMA], blue). Positive staining for alpha-SMA combined with vessel size confirms that the vessels indicated by arrows are arteries. *B*: Representative images showing the absence of CAA in the basilar artery of a 15-month-old SweArc mouse. *C–D*: Representative images showing the complete absence of CAA in both the intraparenchymal vessels and basilar artery of a 15-month-old WT littermate control mouse. Similarly, no parenchymal Aβ is detected in the WT littermate controls. The intensity of the alpha-SMA staining in *B* and *D* was increased using the "Brightness/Contrast" tool in ImageJ to allow proper visualization of the smooth muscle cell layers within the vessel wall. Scale bar in *A* and *C* = 200 μm; in *B* and *D* = 50 μm.

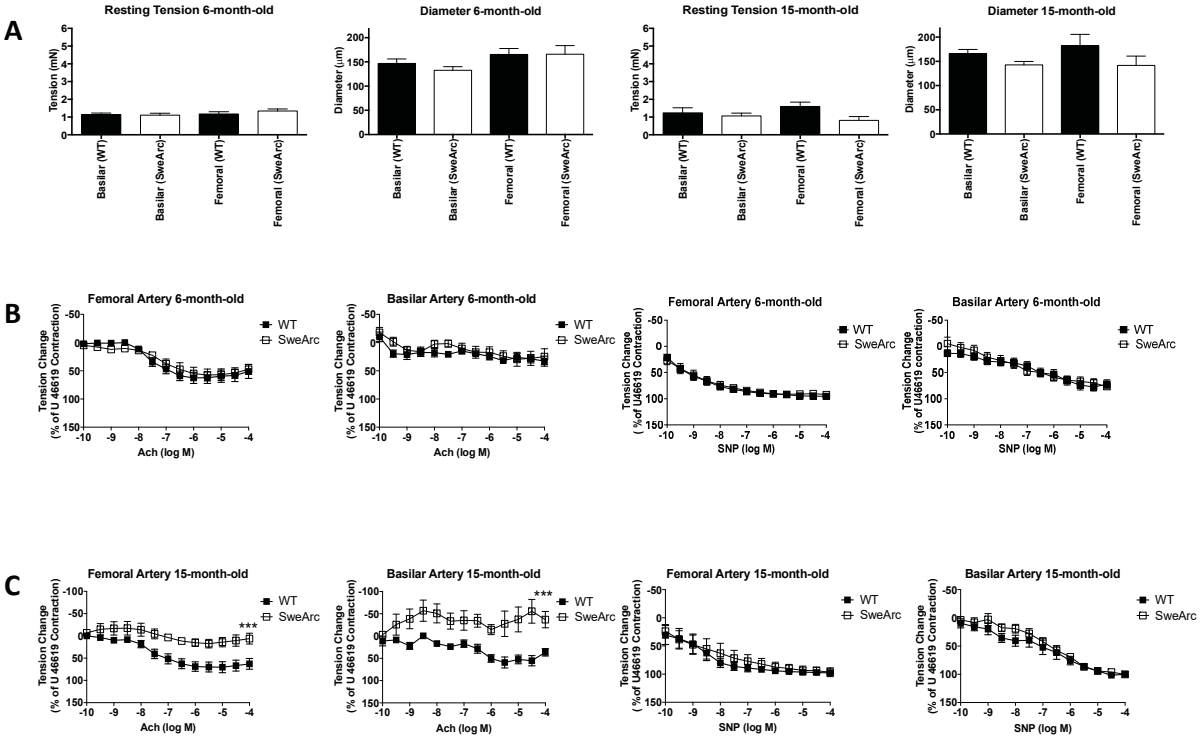
A
Resting Tension 6-month-old
Tension (mN)
Diameter 6-month-old
Diameter (μm)
Resting Tension 15-month-old
Tension (mN)
Diameter 15-month-old
Diameter (μm)
Basilar (WT)
Basilar (SweArc)
Femoral (WT)
Femoral (SweArc)
B
Femoral Artery 6-month-old
Basilar Artery 6-month-old
Femoral Artery 6-month-old
Basilar Artery 6-month-old
Tension Change (% of U 46619 Contraction)
Ach (log M)
SNP (log M)
WT
SweArc
C
Femoral Artery 15-month-old
Basilar Artery 15-month-old
Femoral Artery 15-month-old
Basilar Artery 15-month-old
***

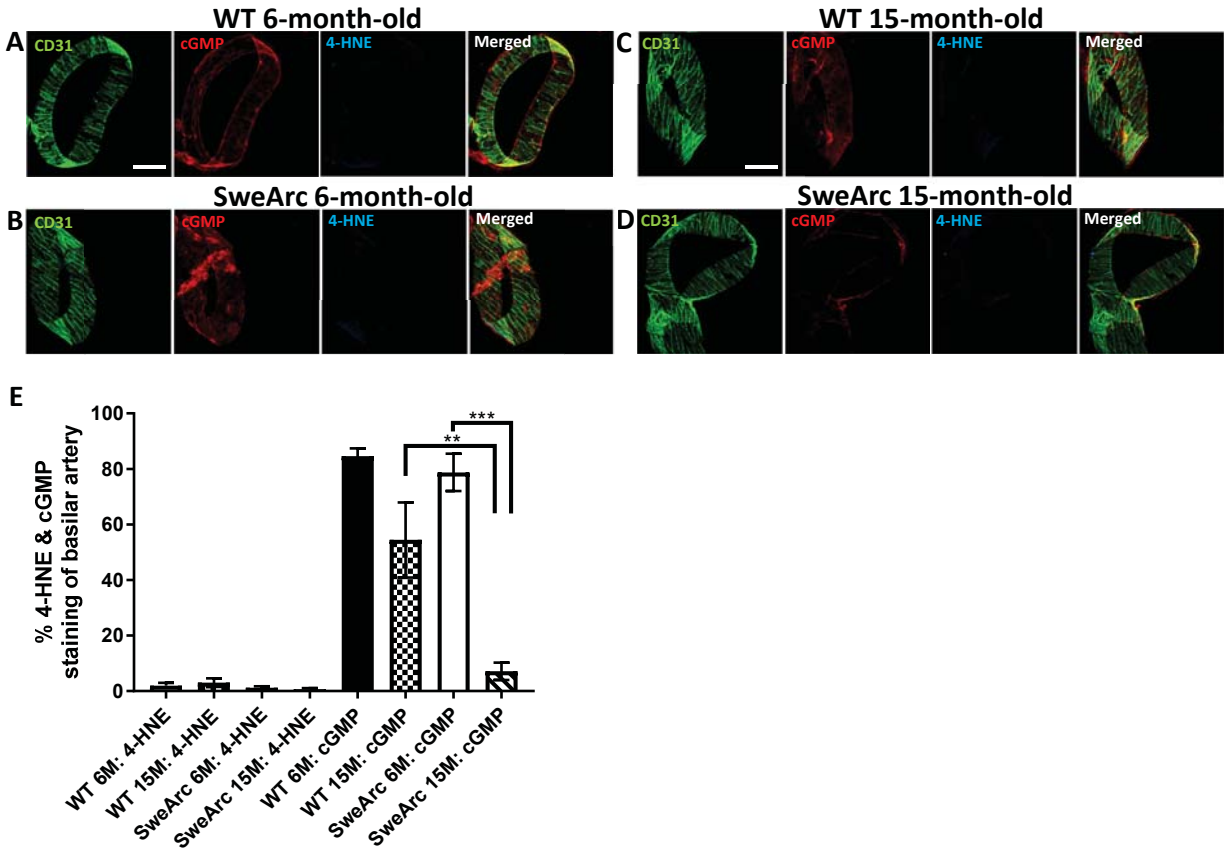
A
WT 6-month-old
CD31
cGMP
4-HNE
Merged
B
SweArc 6-month-old
CD31
cGMP
4-HNE
Merged
C
WT 15-month-old
CD31
cGMP
4-HNE
Merged
D
SweArc 15-month-old
CD31
cGMP
4-HNE
Merged
E
% 4-HNE & cGMP staining of basilar artery
100
80
60
40
20
0
***
**
WT 6M: 4-HNE
WT 15M: 4-HNE
SweArc 6M: 4-HNE
SweArc 15M: 4-HNE
WT 6M: cGMP
WT 15M: cGMP
SweArc 6M: cGMP
SweArc 15M: cGMP

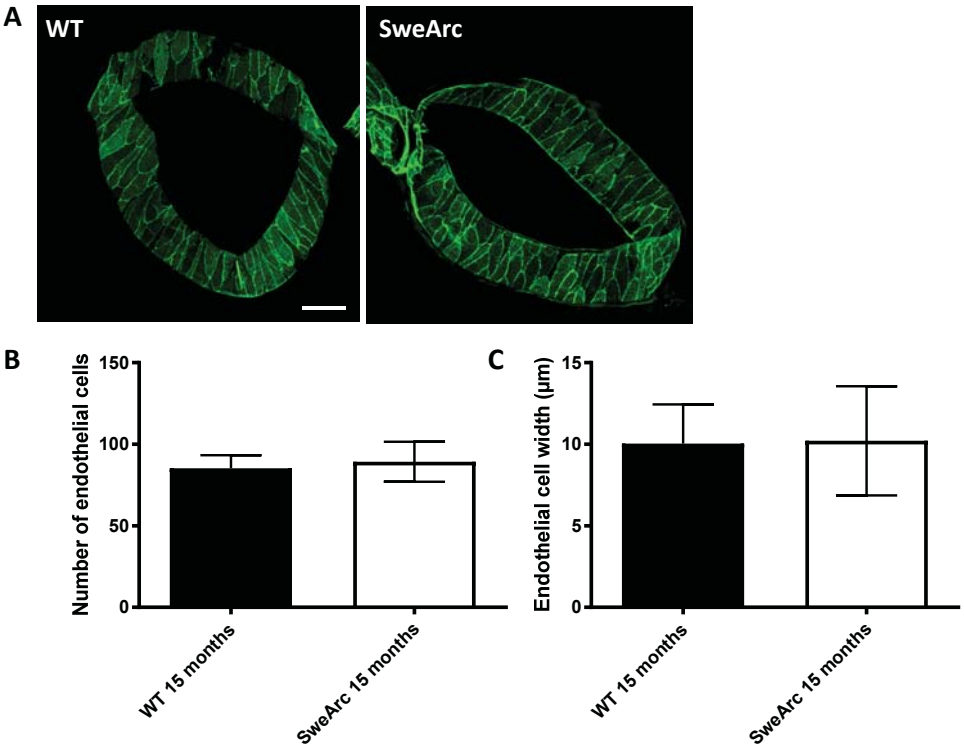
A
WT
SweArc
B
Number of endothelial cells
150
100
50
0
WT 15 months
SweArc 15 months
C
Endothelial cell width (µm)
15
10
5
0
WT 15 months
SweArc 15 months

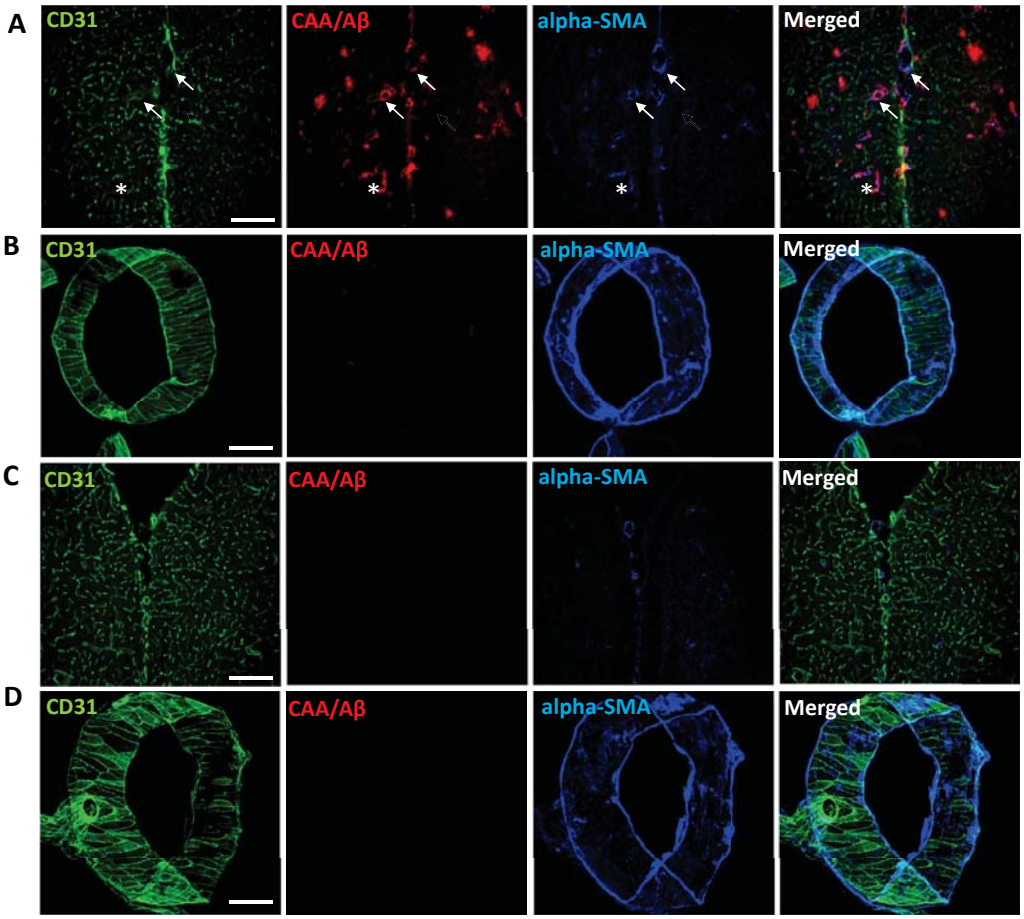
A
CD31
CAA/Aβ
alpha-SMA
Merged
B
CD31
CAA/Aβ
alpha-SMA
Merged
C
CD31
CAA/Aβ
alpha-SMA
Merged
D
CD31
CAA/Aβ
alpha-SMA
Merged